– WGNE Drag Project –
An inter-model comparison of surface stresses

Report no. 1

Ayrton Zadra
Atmospheric Numerical Weather Prediction Research Division
Environment Canada

December 10, 2013

with contributions from

Julio Bacmeister – National Center for Atmospheric Research, USA
Anton Beljaars – European Centre for Medium-Range Weather Forecasts
François Bouyssel – Meteo-France
Andy Brown and Adrian Lock – UK MetOffice
Silvio N. Figueroa and Valdir Innocentini – CPTEC, INPE, Brazil
Masayuki Nakagawa – Japan Meteorology Agency
Greg Roff – Centre for Australian Weather and Climate Research
Mikhail Tolstykh – Russian Academy of Sciences

1 Introduction

The primary goal of this project is to compare parametrizations associated with surface drag, i.e. the schemes currently employed by NWP and climate models to compute subgrid-scale surface stresses and their impact on the atmospheric flow.

At the first Pan-GASS conference[1], Anton Beljaars presented some results[2] comparing surface stresses from the ECMWF and UKMet models and suggested that more work on momentum exchanges could be of interest to all. In fact, the majority of the inter-comparison projects presently under the GASS panel[3] are focussed on thermodynamic and/or microphysics processes, while very few (if any) involve momentum-related parametrizations and processes.

During the 2012 WGNE meeting, the Canadian center report[4] showed an example on recent adjustments to the orographic blocking and boundary layer schemes, and the large-scale forecast improvements that followed. WGNE members therefore agreed to launch a momentum/drag inter-model comparison study, hereafter called Drag Project.

In the first stage of the project, various components of the surface drag (or surface stress) provided by the participating models were to be compared. This report summarizes the results of this preliminary comparison. Details on the requested model data are described in section 2. The main results are shown and discussed in section 3 and in related appendices. A summary of the main findings is provided in section 4. Some ideas for further investigation in future stages of the project may also be found in section 4.

2 Model data

The participating centers and the main characteristics of their models are listed in Table 1. More details about the models may be found in appendix D.

2.1 Basic model output

Using operational (or quasi-operational) configurations of their global models, and initial conditions of their own choice, the participating centers were asked to provide surface stresses averaged over a winter and a summer month.

Here, the term "surface stress"

$$\vec{\tau} \;=\; (\tau_x, \tau_y) \tag{1}$$

refers to the force parallel to the surface, per unit area, as applied by the wind on the earth's surface (land or water). In a forecast model at a given horizontal resolution, the surface

[1] http://www.gewex.org/2012gass_conf.html

[2] http://www.gewex.org/gass/Beljaars.pdf

[3] The Global Atmospheric System Studies (GASS) Panel facilitates and supports the international community who carry out and use observations, process studies and numerical model experiments with the goal of developing and improving the representation of the atmosphere in weather and climate models. Primarily, GASS coordinates scientific projects that bring together experts to contribute to the development of atmospheric models. See http://www.gewex.org/gass_panel.html

[4] http://www.wmo.int/pages/prog/arep/wwrp/new/documents/Zadra_WGNE_28.pdf

stress is partly resolved and partly parametrized,

$$\vec{\tau} = \vec{\tau}^{res} + \vec{\tau}^{phy} \quad (2)$$

$$\vec{\tau}^{res} = p_s \vec{\nabla} h = \text{resolved orographic stress} \quad (3)$$

$$\vec{\tau}^{phy} = \text{subgrid (physics) stress} \quad (4)$$

The main goal of the Drag Projet is to compare the parametrized component of this surface stress, i.e. the stress associated with physics parametrizations such as the planetary boundary layer (PBL) and the subgrid orographic (SGO) schemes.

$$\vec{\tau}^{phy} = \vec{\tau}^{pbl} + \vec{\tau}^{sgo} \quad (5)$$

$$\vec{\tau}^{pbl} = \text{stress from PBL scheme} \quad (6)$$

$$\vec{\tau}^{sgo} = \text{stress from subgrid orographic scheme(s)} \quad (7)$$

Therefore, the participants were asked to submit the x- and y-components of the total parametrized stress, in units of Nm^{-2}, averaged over the first day (24h) of a month of forecasts.

The months proposed were Jan and Jul 2012. Climate models that did not have simulations covering those months provided Jan and Jul averages from the most recent year available.

2.2 Optional model output

Participants were also invited:

- to break down the surface stress into its various contributions (e.g. PBL, gravity-wave drag, low-level blocking, etc.). This partition varies from one model to another, but all models include one PBL scheme and one-or-more orographic schemes (a combination of which defines the model's SGO contribution).
- to produce separate averages over the 00-06, 06-12, 12-18 and 18-24 UTC periods, so that the diurnal cycle of stresses could also be investigated.
- to provide averages of the resolved stress; or, alternatively, the topography elevation and averages of the surface pressure field.
- to provide averages of wind components U and V at 850 hPa.

3 Results

Only the main results and a subset of figures are shown below. The complete set of figures may be found in the Drag Project website[5].

[5] http://collaboration.cmc.ec.gc.ca/science/rpn/drag_project/

3.1 Surface stress maps

Figures 1 and 2 show the 24-h means of the zonal component of the total parametrized (physics) stress, averaged of the winter-month simulations for each model. Similarly, Figures 3 and 4 show the corresponding averages for the summer month. A few features stand out:

- Overall, the models seem to produce similar results over the oceans, regardless of the differences in resolution. The exceptions are the CPTEC's AGCM and AGCM-2 (to be investigated), and UCAR's CAM-5 (possibly due to the different month that this model used to produce the averages).

- There is a fairly good agreement over land, among the NWP models with comparable resolution. Coarser-resolution models (e.g. SL-AV and CAM-5; also ARPEGE in the southern hemisphere) tend to produce higher values of unresolved stress, as expected. Note that the simulations of the CPTEC's AGCM did not use a blocking scheme, which may explain the relatively low values of the stress over land.

Further differences over land become apparent when one compares the stress components terms individually (Figures 5 to 12), especially over the mountaineous regions. Among the high-resolution models:

- compared to the other models, the ECMMF model produces the highest values of PBL stress over mountains, and lowest values of SGO stress;

- the UKMet, JMA and ABOM models exhibit the opposite type of partition, i.e. relatively low (high) values of PBL (SGO) stress;

- whereas the stresses produced by the CMC and MeteoFrance models lie somewhere in between those extremes.

As for the lower-resolution models:

- the magnitude of both the PBL and SGO stresses over land are relatively small in the CPTEC models (recall that, in this case, the SGO stress comes from the GWD scheme only);

- the magnitude of the PBL stress produced by the HMCR model is on the weak side (i.e comparable to that of the JMA model), but its SGO stress is one of the largest;

- of all models, the UCAR's has the lowest values of the PBL stress over land, which is partly compensated by large SGO stresses (Note: one might argue that the stress from the TMS scheme used by CAM-5 should be treated as part of the PBL stress instead of being an SGO component, in which case the figures should be re-generated and this discussion should be revised).

3.2 Zonally averaged torques

According to Brown (2004), the zonal average of the vertically integrated equation for the relative angular momentum may be written as

$$-\frac{\partial}{\partial t}[M_r] = [F] + [C] + [R] + [P] \tag{8}$$

where

$$[\cdots] \quad \text{indicates zonal average} \tag{9}$$

$$M_r = a\cos\phi \int_0^{p_s} u\frac{dp}{g} = \text{integrated relative angular momentum} \tag{10}$$

$$F = \frac{1}{\cos\phi}\frac{\partial}{\partial\phi}\left(\cos^2\phi \int_0^{p_s} uv\frac{dp}{g}\right) = \text{flux convergence term} \tag{11}$$

$$C = fa\cos\phi \int_0^{p_s} v\frac{dp}{g} = \text{Coriolis term} \tag{12}$$

$$R = a\cos\phi\,\tau_x^{res} = \text{resolved surface pressure torque} \tag{13}$$

$$P = a\cos\phi\,\tau_x^{phy} = \text{unresolved (physics) torque} \tag{14}$$

$$\tau_x^{res} = \frac{p_s}{a\cos\phi}\frac{\partial h}{\partial\lambda} = \text{zonal component of resolved stress} \tag{15}$$

$$\tau_x^{phy} = \text{zonal component of unresolved (physics) stress} \tag{16}$$

and where t, λ, ϕ, p represent time, longitude, latitude and pressure, respectively; a is the earth's radius, g the gravity constant, f the Coriolis parameter, u, v the zonal and meridional components of the wind field, p_s the surface pressure, and h the topography elevation. Note that R and P have units of $N \cdot m^{-1}$, i.e. they actually give the torque per unit area.

To produce the zonally averaged torques in $N \cdot m$ shown in figs. 13 and 14, the quantities $[R]$ and $[P]$ (and the separate terms and contributions to $[P]$) were multiplied by $a^2\cos\phi$ – or equivalently, the zonally averaged stresses $[\tau]$ were multiplied by $a^3\cos^2\phi$ (see appendix B for a justification to this procedure). Note that the curves were smoothed using a 5^o-mean filter. Note also that results from the ACCES and CAM5 models are not shown here, since ACCES did not provide SGO stresses and CAM5 results come from a different month.

The comparison of zonally averaged torques (figs. 13 and 14) confirms some of the similarities and differences discussed in the previous section, but allows us to further quantify some of those differences:

- For the PBL torque over water, there is an approximate consensus among the majority models. The exceptions are the two versions of the CPTEC's AGCM (whose PBL torque values can be 30 to 40% smaller than the consensus), and MeteoFrance's ARPEGE (whose peak values of the torque are 10 to 20% smaller than the consensus).

- Over land, especially over the northern latitudes in winter, the spread among the model torques is more pronounced. This is true for both the PBL and SGO components of the torque, where the ratio between different model results may be as high as 2 or 3. In this case, models that show relatively large values of PBL torque also show small values of SGO torque, and vice-versa (the CPTEC models being the only exception).

3.3 Zonal average of stress magnitude

Note that the calculation of torques discussed in the previous section only depends on the x-component of the stresses. Moreover, positive and negative contributions to the torque may cancel out when we produce zonal averages. To complement the findings of section 3.2, we here compare the zonal averages of the stress magnitude and its components (see appendix C for calculation details).

Results are shown in figs. 15 and 16 where, as in the previous section, all curves have been smoothed using a 5^o-mean filter. The conclusions are similar to those of section 3.2, although the differences between model results are somewhat enhanced when we compare the stress magnitudes:

- The spread of solutions for the stress magnitude is larger over land than over water.
- Among the high-resolution models, the UKMetO and has the largest values of SGO stresses. In midlatitudes, the magnitude of the SGO stresses of the IFS and ARPEGE models can be 4 to 5 times smaller than those of the UKMetO model.
- Conversely, the PBL stresses over land of the IFS and ARPEGE models can be twice as large as those of the other high-resolution models.
- Recall that the physics (PBL+SGO) torques of the high-resolution models were quite similar (Fig. 13). This does not hold anymore when we compare the magnitude of the physics (PBL+SGO) stresses for which the spread is not negligeable in both seasons (Figs. 15 and 16).

3.4 Diurnal cycle

The results and the discussion presented so far have been focussed on the 00-24h averages. To illustrate stress variations within the diurnal cycle of each model, Figure 17 shows the zonal mean of the physics torque for Jan 2012, averaged separately over the 00-06, 06-12, 12-18 and 18-24h periods.

In spite of some local oscillations in the stress amplitude (e.g. within the $0 - 20^oN$ latitudinal band), the similarities and differences mentioned in the previous sections appear to be true for any of the 6h periods. A model detailed analysis of the diurnal cycle of stresses remains to be done.

4 Summary

The surface stresses produced by ten different models were compared. For the participating NWP models, the stresses provided correspond to averages over the months of January and July 2012, derived from 00-24h forecasts. These stresses were further decomposed into contributions from different parametrizations (e.g. PBL and SGO schemes), different surfaces (water and land) and separate 6-h periods of the day, and the associated zonal averages (stresses and torques) were produced.

Overall, the largest differences among the model stresses are found over land. Even when two models produce similar values for the total parametrized stress, they may disagree on the values of the individual (PBL and SGO) components. Only a fraction of these differences may be attributed to differences in horizontal resolution, since some of the models have similar resolution and yet seem to generate different stresses. Other factors such as surface parameters (e.g. ancillary fields) and differences in the scheme formulations (e.g. dependence on stability) may play a role and remain to be investigated.

In contrast, there is less spread in the results for the stress over water (which comes from the PBL scheme only) except for the CPTEC and MeteoFrance models (whose stresses tend to be weaker than the other models) and the HMCR model (which seems to produce relatively weak stresses over water, except over the southern extra-tropics).

The results presented here are preliminary in as much as no attempt was made to explain the differences found among the models stresses. This is left for future stages of the project, since it will probably require access to details on the individual parametrizations and to other input fields (such as upper-air profiles of winds and static stability). It might also be useful to compare the actual profiles of physics tendencies generated by the models, although that brings up the challenge of choosing the most appropriate vertical coordinate for the comparison of tendencies.

We might also consider developing a single column model (SCM) protocol with prescribed forcings to compare the stresses produced by different schemes in a simple and controlled manner (to be discussed).

Finally, once we agree with a more complete set of output fields and diagnostics, we might want to extend the invitation to other models/centers (other than the current WGNE members) to participate in this exercise.

Appendices

A Notation

In some of the figures and tables, the following notation has been used:

(i) vector components and magnitude of stress

tau**x**??? = u-component of surface stress
tau**y**??? = v-component of surface stress
tau**m**??? = magnitude of surface stress = $\sqrt{(taux???)^2 + (tauy???)^2}$

(ii) physics and dynamics contributions to the stress

tau?**pbl** = stress from PBL scheme
tau?**sgo** = stress from all subgrid orographic schemes combined
tau?**phy** = stress from physics = (tau?pbl + tau?sgo)
tau?**gwd** = stress from orographic gravity-wave drag (GWD) scheme
tau?**blc** = stress from orographic blocking scheme
tau?**lwg** = stress from long-wave GWD scheme[6]
tau?**swg** = stress from short-wave GWD scheme[7]
tau?**tms** = stress from turbulent mountain stress (TMS) scheme[8]
tau?**res** = resolved orographic stress

(iii) wind field at 850hPa

uu850mb = u-component of wind at 850hPa
vv850mb = v-component of wind at 850hPa
uv850mb = wind speed at 850hPa = $\sqrt{(uu850)^2 + (vv850mb)^2}$

[6]Used by the JMA GSM model.
[7]Used by the JMA GSM model.
[8]Used by the UCAR CAM-5 model.

B Zonal averages of torques

The surface average of a field A defined over the globe can be written as

$$\int_{globe} A dS = \int_{-\pi/2}^{\pi/2}\int_{0}^{2\pi} A a^2 \cos\phi \, d\lambda d\phi \tag{17}$$

$$= \int_{-\pi/2}^{\pi/2} \left([A] a^2 \cos\phi\right) 2\pi d\phi \tag{18}$$

where $[A]$ is the zonal mean of A. In the case of the physics torque per unit area P, for instance, this implies:

$$\text{physics torque} = \int_{globe} P dS \tag{19}$$

$$= \int_{-\pi/2}^{\pi/2} [\tau_x^{phy} a \cos\phi] a^2 \cos\phi \, 2\pi d\phi \tag{20}$$

$$= \int_{-\pi/2}^{\pi/2} \left([\tau_x^{phy}] a^3 \cos^2\phi\right) 2\pi d\phi \tag{21}$$

This justifies the calculations used in the production of figs. 13, 14 and 17, i.e. why the stress component τ_x has been multiplied by $a^3 \cos^2\phi$ and why the resulting quantity has units of $N \cdot m$.

Zonal averages of the stress field were also decomposed as the sum of land and water contributions:

$$[\tau] = [\tau]^{land} + [\tau]^{water} \tag{22}$$

$$[\tau]^{land} = [\tau \cdot s_l] = \text{contribution from land to } [\tau] \tag{23}$$

$$[\tau]^{water} = [\tau \cdot (1 - s_l)] = \text{contribution from water to } [\tau] \tag{24}$$

$$s_l(\lambda, \phi) = \begin{cases} 1 & \text{, if land fraction of grid cell exceeds } 50\% \\ 0 & \text{, otherwise} \end{cases} \tag{25}$$

The fraction of land/water of each grid cell was estimated using the land/water-fraction field of the Canadian model, interpolated onto the grid of each model (this interpolation was performed using the matlab function *interp2*).

C Zonal averages of stresses

The zonal average of the stress components and magnitude were also averaged over land and water grid cells separately:

$$[\tau]^{l-avg} = \frac{[\tau \cdot s_l]}{[s_l]} = \text{stress averaged over land grid cells} \tag{26}$$

$$[\tau]^{w-avg} = \frac{[\tau \cdot (1 - s_l)]}{[(1 - s_l)]} = \text{stress averaged over water grid cells} \tag{27}$$

from which the total stress may be re-obtained as a weighted sum,

$$[\tau] = [s_l] \cdot [\tau]^{l-avg} + [(1 - s_l)] \cdot [\tau]^{w-avg} \tag{28}$$

where $[s_l]$ ($[(1-s_l)]$) gives the zonally-averaged fraction of the surface covered by land (water).

D Further information on the participating centers and models

D.1 GDPS from the Canadian Meteorological Centre (CMC)

- Model name: GDPS (Global Deterministic Prediction System; CMC Technical Report, 2013).
- Spatial resolution: 0.35^ox0.2^o lat-lon, 80 levels, top at 0.1 hPa.
- PBL scheme: Turbulent kinetic energy 1.5-order closure scheme (Bélair et al. 1999, Bougeault and Lacarrère 1989).
- SGO scheme: Orographic GWD scheme based on McFarlane (1987) and low-level blocking based on Lott and Miller (1997), Vosper et al. (2009) and Wells et al. (2008).

D.2 GSM from the Japan Meteorological Agency (JMA)

- Model name: Global Spectral Model (GSM: JMA, 2013)
- Spatial resolution: TL959L60 (approximately 20 km in the horizontal and 60 layers up to 0.1 hPa in the vertical)
- PBL scheme: Mellor-Yamada level 2 (Mellor and Yamada, 1974)
- GWD scheme: Longwave scheme (wavelengths $>$ 100 km) and shortwave scheme (wavelengths approx. 10 km) based on Iwasaki et al. (1989)

D.3 SL-AV from the Hydrometeorological Research Centre of Russia (HMCR)

- Model name: SL-AV (Tolstykh, 2010 [Russian], early version Tolstykh, Russ. Meteor. and Hydrol. 2001)
- Spatial resolution: 0.72x0.9 lat-lon, 28 levels. Vorticity-divergence SISL dynamical core of own development (description in English is also in (Shashkin, Tolstykh 2013 doi: 10.5194/gmdd-6-4809-2013), ALADIN/LACE parameterizations (www.rclace.eu).
- PBL scheme: Pseudo prognostic TKE scheme (J.-F. Geleyn *et al.*, 2006).
- SGO scheme: It describes in a broad sense the influence of unresolved orography on the higher levels of the atmosphere in a way adapted from Boer et al. (1984) for the linear gravity wave drag part (with full use of the Lindzen (1981) saturation criterion for applying the Eliassen-Palm theorem) and from Lott and Miller (1997) for the form drag low level part. A parameterisation of the sub-grid scale so-called lift effect exists, following Lott (1999). Some additional effects are taken into account for the following aspects: (i) influence of the anisotropy of the sub-grid orography on the direction

and intensity of the stress, according to Phillips (1984); (ii) use of averaged wind and stability low level conditions (and smooth return to the true profiles above the averaging depth) in order to get a surface stress as independent as possible of the model's vertical discretisation; (iii) amplifying or destructive resonance effects parameterised according to the work of Peltier and Clark (1986), as well as dispersion effects in case of upper-air neutrality.

D.4 ARPEGE from Meteo-France

- Model name: Arpege
- Spatial resolution: T798 stretching factor 2.4 which corresponds to 10.5km over France and 60km over antipodes. 70 vertical levels (lowest model level at 17m, model top at 0.1 hPa). Time-step is 514s.
- PBL scheme: The prognostic TKE turbulent scheme (Cuxart et al., 2000) is used with Bougeault and Lacarrre (1989) mixing length. The surface exchange coefficient are computed according to Louis et al. (1982) formulation using an effective mixing length (including subgrid orography contribution).
- SGO scheme: The parameterization of subgrid orographic effects is described in the annexe of Catry et al. (2008) paper. It takes into account surface GWD (Boer et al., 1984), orographic anisotropy, Lindzen saturation (1981), resonance (Peltier et Clark, 1986) and blocking effects (Lott et Miller, 1995).

D.5 GM from the UK Met Office

- Model name: Global (GM) configuration of the Met Office Unified Model
- Spatial resolution: 0.35^ox0.23^o lat-lon, 70 levels, top at 80 km.
- PBL scheme: First-order K-profile closure with explicit entrainment parametrization, and nonlocal mixing in unstable layers (Lock et al. 2000; Lock 2001; Brown et al. 2008)
- SGO scheme: Flow-blocking and gravity-wave drag parametrization (Webster et al. 2003, Brown and Webster 2004) representing the effect of orography on scales between about 5 km and the model grid-scale.

D.6 IFS from the European Centre for Medium-Range Weather Forecasts (ECMWF)

- Model name: Integrated Forecasting System (IFS).

  Documentation: http://www.ecmwf.int/research/ifsdocs/CY38r1/

  The model version for Jan 2012 is CY37R3, which was changed to CY38R1 on 19 June 2012. None of the changes were relevant for the surface drag.

- Spatial resolution: The model has a spectral resolution of T1279 with a resolution of about 16 km in grid point space. The reduced Gausssian Grid decreases the number of grid points towards the poles such that the grid point spacing is similar over the entire globe.

- PBL scheme: A first order diffusion/mass flux scheme is used for the convective boundary layer (Koehler at al. 2011). In the stable regime a revised Louis scheme is used with a long-tail stability function near the surface and a Monin-Obukhov type function (short-tails) above the boundary layer (see Bechtold et al. 2008). The ocean roughness is controlled through a two-way interaction with an ocean wave model (Documentation: http://www.ecmwf.int/research/ifsdocs/CY38r1/). Over land the surface roughness is controlled by vegetation type / land use on the basis of the GLCC climatological data set. Roughness length is coupled to the 20 GLCC vegetation types through an empirical correspondence table. The model does not have an orographic contribution to roughness length. Instead the Turbulent Orographic Form Drag (TOFD) is implemented as a separate process that puts a drag profile on model levels (Beljaars et al. 2004). The turbulent drag and the drag from the TOFD scheme are post-processed and diagnosed together, so the combination is called "turbulent drag".

- SGO scheme: The Subgrid Orography scheme (SO) has two components: A blocking scheme that provides low level drag and and a gravity wave component that provides drag through propagating gravity waves at a breaking level higher up in the atmosphere. For details see Lott and Miller (1997). Some of the coefficients have been adjusted compared to the paper.

D.7 ACCESS from the Australian Bureau of Meteorology (BOM)

- Model name: ACCESS-G1 (the Global configuration of the Australian Community Climate and Earth-System Simulator (ACCESS) upgraded to Australian Parallel Suite 1

- Spatial resolution: N320 (i.e. 481 latitude x 640 longitude gridpoints = 0.3750 x 0.5625 or a nominal grid spacing of approximately 40km) and 70 vertical levels, top level at approximately 80km (0.009 hPa)

- PBL scheme: Mixing in unstable layers uses the first order non-local scheme of Lock et al. (2000) that parameterises eddy diffusivity profiles of unstable (well-mixed) layers driven either by fluxes at the surface or by cloud-top processes. However, for scalar variables, APS1 no longer uses calculations of individual flux components to determine the total flux. Instead, a revised formulation determines fluxes of scalar variables in terms of a total flux and a non-turbulent component with the difference being the turbulent flux. Revisions were also made to the specification of cloud-top entrainment to avoid spurious jumps in the scalar profiles across the inversion. APS1 also uses a preliminary version of a new temperature decoupling parameterization devised to better represent screen-level temperatures and humidities under light winds and strong surface cooling (Edwards et al., 2011). This has been shown to limit over-predictions of screen-level

dewpoint temperatures over inland Australia during the evening transition. Boundary layers are classified according to 7 separate types with unstable layers identified using a parcel ascent/descent method. Cumulus mixing uses the mass-flux convection scheme. Entrainment rates across the inversion at the top of the boundary layer are specified using an eddy diffusivity scheme of Lock (1998; 2000) scaled using cloud-top cooling rates. Mixing in stable boundary layers uses the local Richardson number first order closure of Louis (1979) with stability depe

- SGO scheme: The model has orographic and spectral gravity wave schemes (Webster, 2003, 2004; Warner and McIntyre, 1996, 2001). The orographic gravity wave scheme allows for blocking as well as gravity wave drag and has been shown to improve the general circulation. Similarly the spectral scheme has been shown to improve the simulation of the tropical stratosphere and high latitude features such as the southern winter jet.

D.8 ACGM and AGCM2 from the Centro de Previsão de Tempo e Estudos Climáticos (CPTEC)

- Model name: CPTEC AGCM-V.4.0
- Spatial resolution: T299L64 (approximately 45 km in the horizontal and 64 vertical levels).
- PBL scheme: The modified nonlocal Melhor-Yamada level 2 scheme (Melhor and Yamada, 1974).
- GWD scheme: AGCM1 used the Alpert et al. (1998) scheme, where the surface wind stress is a nonlinear function of the wind speed and the local Froud Number. And AGCM2 used the hybrid Webster et al. (2003) scheme which leads with low-level blocking and gravity-wave drag parameterization.

D.9 CAM-5 from the University Corporation for Atmospheric Research (UCAR)

- Model name: Community Atmosphere Model version 5 (CAM 5)
- Spatial resolution: Horizontal, approximately 100km; Vertical, 60 layers, DZ linearly increasing from around 100 meters at the surface to around 500 m at z=1500 meters. Expanding again in top 5 layers to place model top around 40 km.
- PBL scheme: Bretherton and Park (2009). A Diagnostic TKE based (Turbulent Kinetic Energy, e) 1st order K-diffusion scheme with entrainment parameterization but without counter-gradient transport. Explicit cloud-radiation-turbulence interactions with driving by cloud LW radiative cooling.
- GWD scheme: Vertically-propagating orographic gravity waves McFarlane (1987) forced by subgrid topographic variance with scales longer than 5km. In addition, form drag

from smaller scale obstacles is parameterized as an enhanced roughness length in the model's turbulent surface drag scheme. This is referred to as "Turbulent Mountain Stress" (TMS) and is described in Richter et al (2010).

References

[1] Bechtold P., M. Koehler, T. Jung, F. Doblas-Reyes, M. Leutbecher, M. Rodwell, F. Vitart, and G. Balsamo, 2008: Advances in simulating atmospheric variability with the ECMWF model: From Synoptic to decadal time-scales, *Q. J. R. Meteorol. Soc.*, **134**, 1337-1351.

[2] Brown, A.R., 2004: Resolution dependence of orographic torques. *Q. J. R. Meteorol. Soc.*, **130**, pp. 3029-3046.

[3] Brown, A.R. and S. Webster, 2004: Orographic flow-blocking scheme characteristics, *Q. J. R. Meteorol. Soc.*, **130**, 3015-3028.

[4] Brown, A.R., R.J. Beare, J.M. Edwards, A.P. Lock, S.J. Keogh, S.F. Milton and D.N. Walters, 2008: Upgrades to the Boundary-Layer Scheme in the Met Office Numerical Weather Prediction Model. *Boundary-Layer Meteor.*, **128**, 117-132.

[5] Bélair, S., J. Mailhot, J.W. Strapp, and J.I. MacPherson, 1999: An examination of local versus nonlocal aspects of a TKE-based boundary layer scheme in clear convective conditions. *J. Appl. Meteor.*, **38**, 1499-1518.

[6] Beljaars, A.C.M., A.R. Brown and N. Wood, 2004: A new parametrization of turbulent orographic form drag, *Q. J. R. Meteorol. Soc.*, **130**, 1327-1347.

[7] Bougeault, P. and P. Lacarrère, 1989: Parameterization of orography-induced turbulence in a mesobeta-scale model. *Mon. Wea. Rev.*, **117**, 1872-1890.

[8] Bretherton, C. S., and S. Park, 2009: A new moist turbulence parameterization in the community atmosphere model, *J. Climate*, **22**, 34223448.

[9] Catry, B., J.-F. Geleyn, F. Bouyssel, J. Cedilnik, R. Brozkova, M. Derkova and R. Mladek, 2008: A new sub-grid scale lift formulation in a mountain drag parameterisation scheme, *Meteorologische Zeitschrift*, **17**, N.2, pp. 193-208(16).

[10] Canadian Meteorological Centre, 2013: Improvements to the Global Deterministic Prediction System (GDPS): from version 2.2.2 to 3.0.0. Technical Report. http://collaboration.cmc.ec.gc.ca/cmc/cmoi/product_guide/docs/lib/op_systems/doc_opchanges/technote_gdps300_20130213_e.pdf

[11] Cuxart, J., Ph. Bougeault and J-L. Redelsperger, J-L., 2000 : A turbulence scheme allowing for mesoscale and large-eddy simulations, *Q. J. R. Meteorol. Soc.*, **126**, p.1-30.

[12] Edwards, J.M., J.R. McGregor, M.R. Bush and F.J. Bornemann, 2011: Assessment of numerical weather forecasts against observations from Cardington: seasonal diurnal cycles of screen-level and surface temperatures and surface fluxes, *Q. J. R. Meteorol. Soc.* **137**: 656672. DOI:10.1002/qj.742

[13] Geleyn, J.-F., F. Vana, J. Cedilnik, M. Tudor, B. Catry, 2006: An intermediate solution between diagnostic exchange coefficients and prognostic TKE methods for vertical turbulent transport. WGNE Blue Book.

[14] Geleyn, J.-F. and Coauthors, 1995: Atmospheric parametrization schemes in Meteo-France's ARPEGE NWP. Proc. 1994 ECMWF Seminar on Physical Parameterizations in Numerical Models. Reading, United Kingdom, ECMWF, 385-402.

[15] Iwasaki, T., S. Yamada, and K. Tada, 1989: A parameterization scheme of orographic gravity wave drag with two different vertical partitionings, Part I: Impact on medium-range forecasts. *J. Meteor. Soc. Japan*, **67**, 11-27.

[16] Outline of the operational numerical weather prediction at the Japan Meteorological Agency. Appendix to WMO Technical Progress Report on the Global Data-processing and Forecasting System and Numerical Weather Prediction Research. Japan Meteorological Agency, Tokyo, Japan. http://www.jma.go.jp/jma/jma-eng/jma-center/nwp/outline2013-nwp/index.htm

[17] Koehler, M., M. Ahlgrimm and A. Beljaars, 2011: Unified treatment of dry convective and stratocumulus-topped boundary layers in the ECMWF model, *Q. J. R. Meteorol. Soc.*, **137**, 43-57.

[18] Lock A. P., 1998: The Parameterization of entrainment in cloudy boundary layers, *Q. J. R. Meteorol. Soc.*, **124**, 2729-2753.

[19] Lock A. P., A. R. Brown, M. R. Bush, G. M. Martin and R. N. B. Smith, 2000: A new boundary layer mixing scheme. Part I: Scheme description and single-column Model. *Mon. Wea. Rev.*, **128**, 3187-3199.

[20] Lock A. P., 2001: The numerical representation of entrainment in parametrizations of boundary layer turbulent mixing. *Mon. Wea. Rev*, **129**, 1148-1163.

[21] Lott, F. and M.J. Miller, 1997: A new subgrid-scle orographic drag parametrization: Its formulation and testing. *Q. J. R. Meteorol. Soc.*, **123**, 2353-2393.

[22] Louis, J. F., M. Tiedtke and J.F. Geleyn, 1982: A short history of the operational PBLparametrization at ECMWF. Workshop on boundary layer parametrization, November 1981, ECMWF, Reading, England.

[23] McFarlane, N. A., 1987: The effect of orographically excited gravity-wave drag on the circulation of the lower stratosphere and troposphere. *J. Atmos. Sci.*, **44**, 1175-1800.

[24] Mellor, G. L. and T. Yamada, 1974: A hierarchy of turbulence closure models for planetary boundary layers. *J. Atmos. Sci.*, **31**, 1791-1806.

[25] Richter, J. H., F. Sassi, and R. R. Garcia, 2010: Towards a physically-based wave source parameterization in a general circulation model, *J. Atmos. Sci.*, **67**, 136156.

[26] Vosper, S.B., H. Wells and A. R. Brown, 2009: Accounting for non-uniform static stability in orographic drag parametrization. *J. R. Meteorol. Soc.*, **135**, 815-822.

[27] Warner, C.D. and McIntyre, M.E., 1996: On the Propagation and Dissipation of Gravity Wave Spectra through a Realistic Middle Atmosphere. *J. Atmos. Sci.*, **53**, 3213-3235.

[28] Warner, C.D. and McIntyre, M.E., 2001: An Ultrasimple Spectral Parameterization for Nonorographic Gravity Waves. *J. Atmos. Sci.*, **58**, 1837-1857.

[29] Webster, S., Brown, A.R., Cameron, D.R. and Jones, C.P., 2003: Improvements to the representation of orography in the Met. Office Unified Model. *Q. J. R. Meteorol. Soc.*, **129**, 1989-2010.

[30] Webster, S., 2004: Gravity Wave Drag, Unified Model Documentation Paper No. 22.

[31] Wells, H., S. B. Vosper, A. N. Ross, A. R. Brown and S. Webster, 2008: Wind direction effects on orographic drag. *Q. J. R. Meteorol. Soc.*, **134**, 689-701.

Table 1: Participating models

model name	resolution	center	stress components provided
GDPS	25km	CMC	pbl, gwd, blc, res
ARPEGE	10-60km	Meteo-France	pbl, sgo
GM	25km	UK MetOffice	pbl, sgo
IFS	15km	ECMWF	pbl, sgo, res
GSM	20km	JMA	pbl, lgw, sgw, res
ACCESS	40km	Australian BOM	pbl, gwd, blc
AGCM	45km	CPTEC	pbl, gwd, res
AGCM-2	45km	CPTEC	pbl, gwd, res
SL-AV	80km	HMCR	pbl, sgo
CAM-5	100km	UCAR	pbl, gwd, tms

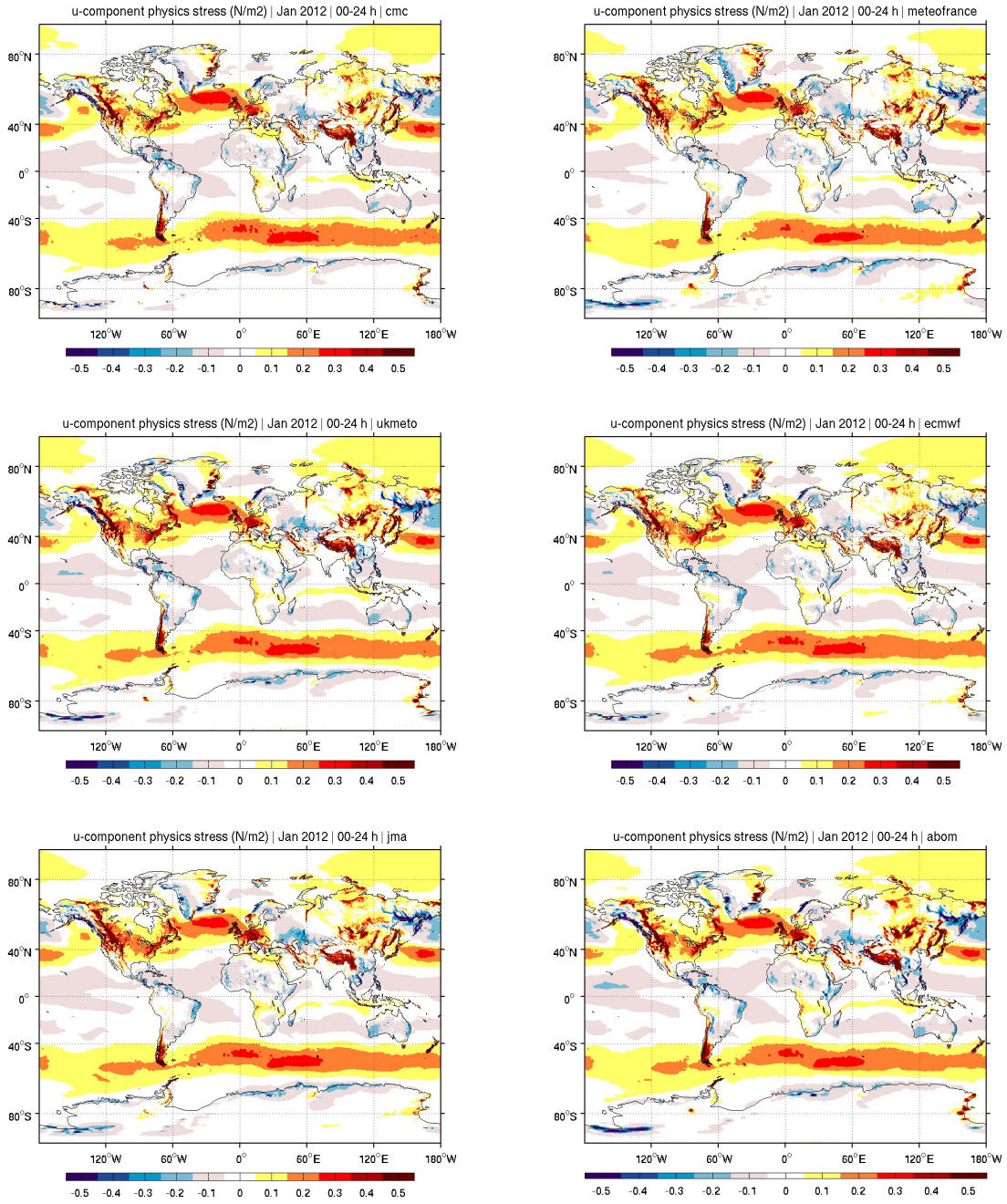

Figure 1: 24-h averages (00-24 UTC) of the u-component of the total subgrid stress (in Nm^{-2}) for Jan 2012, for 6 of the participating centers/models.

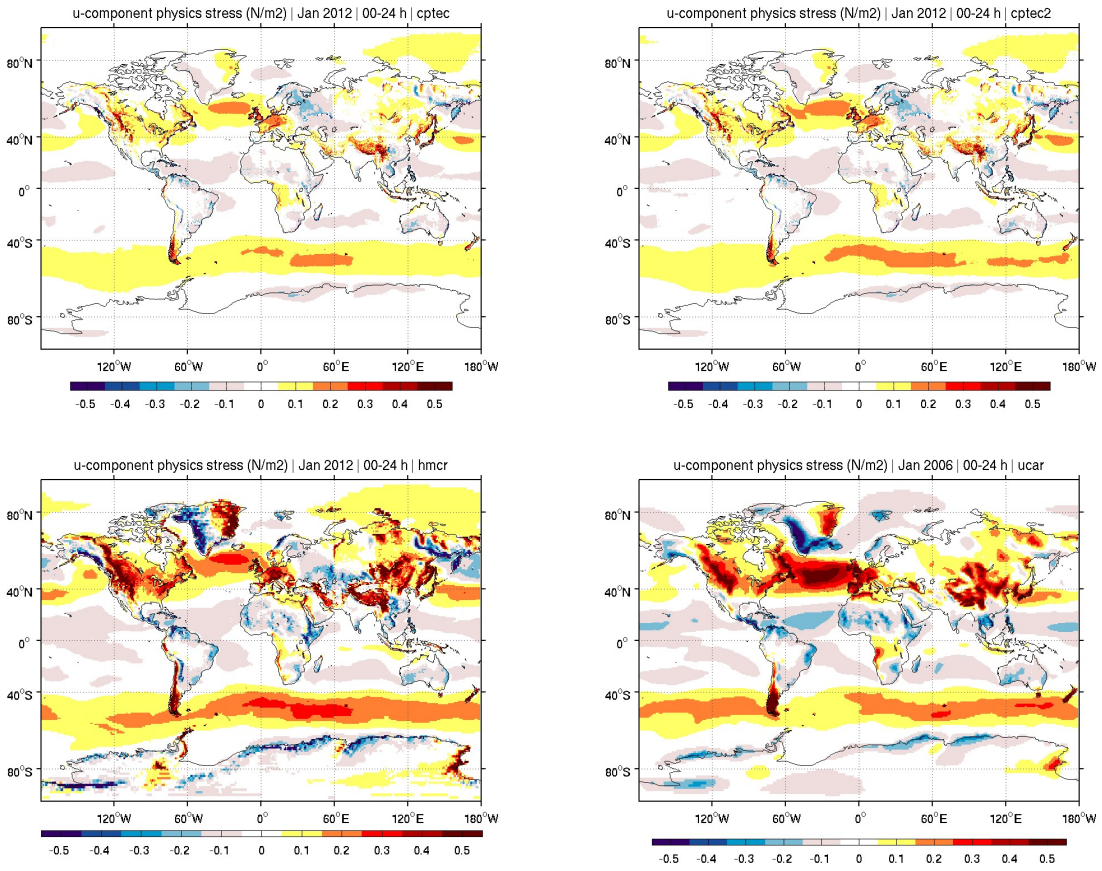

Figure 2: Same as in fig.1, for 4 more models.

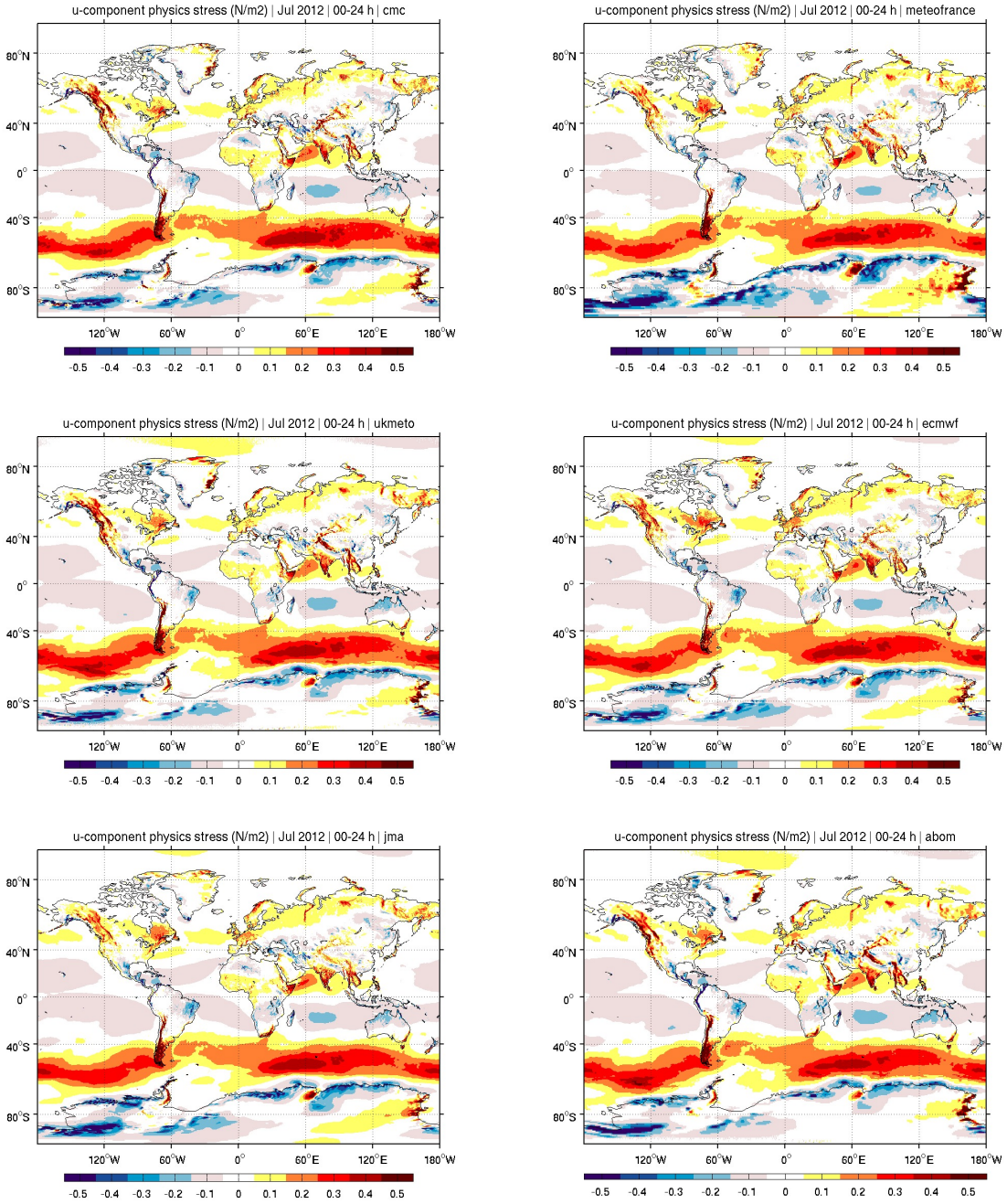

Figure 3: Same as in fig.1, for the month of Jul 2012.

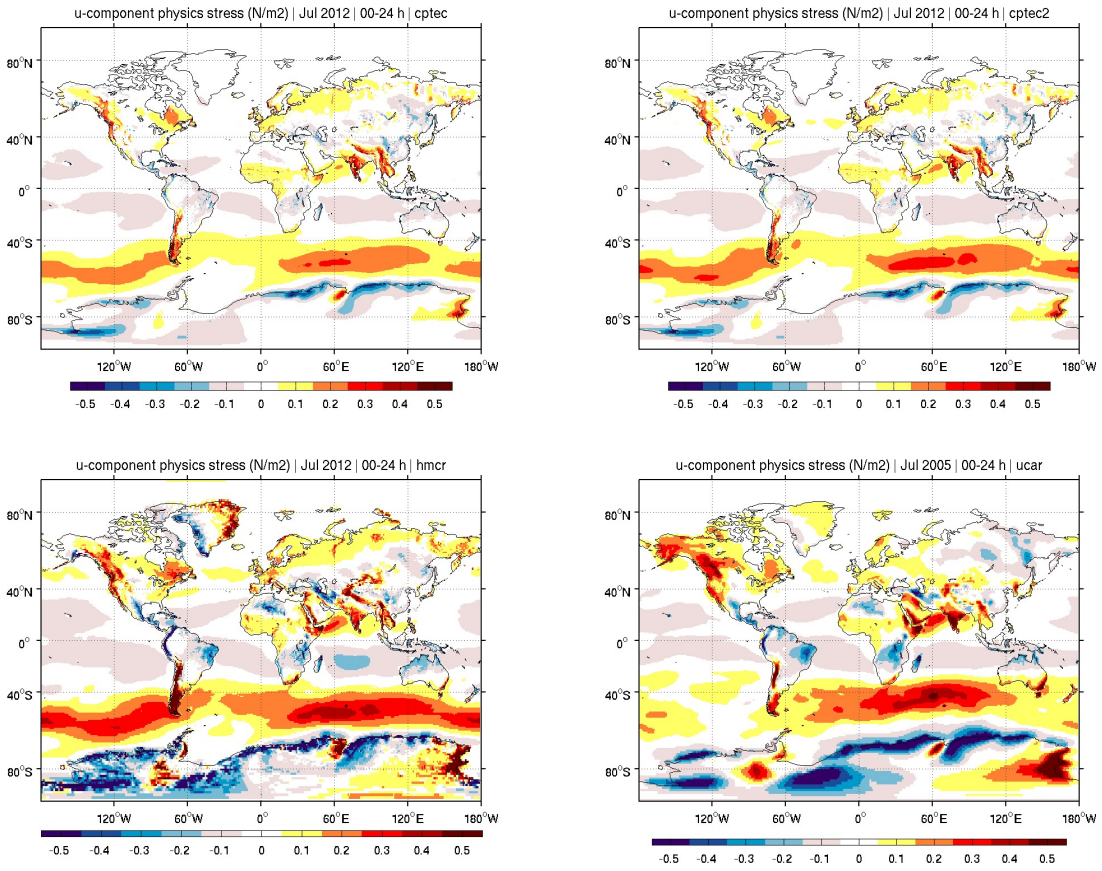

Figure 4: Same as in fig.3, for 4 more models.

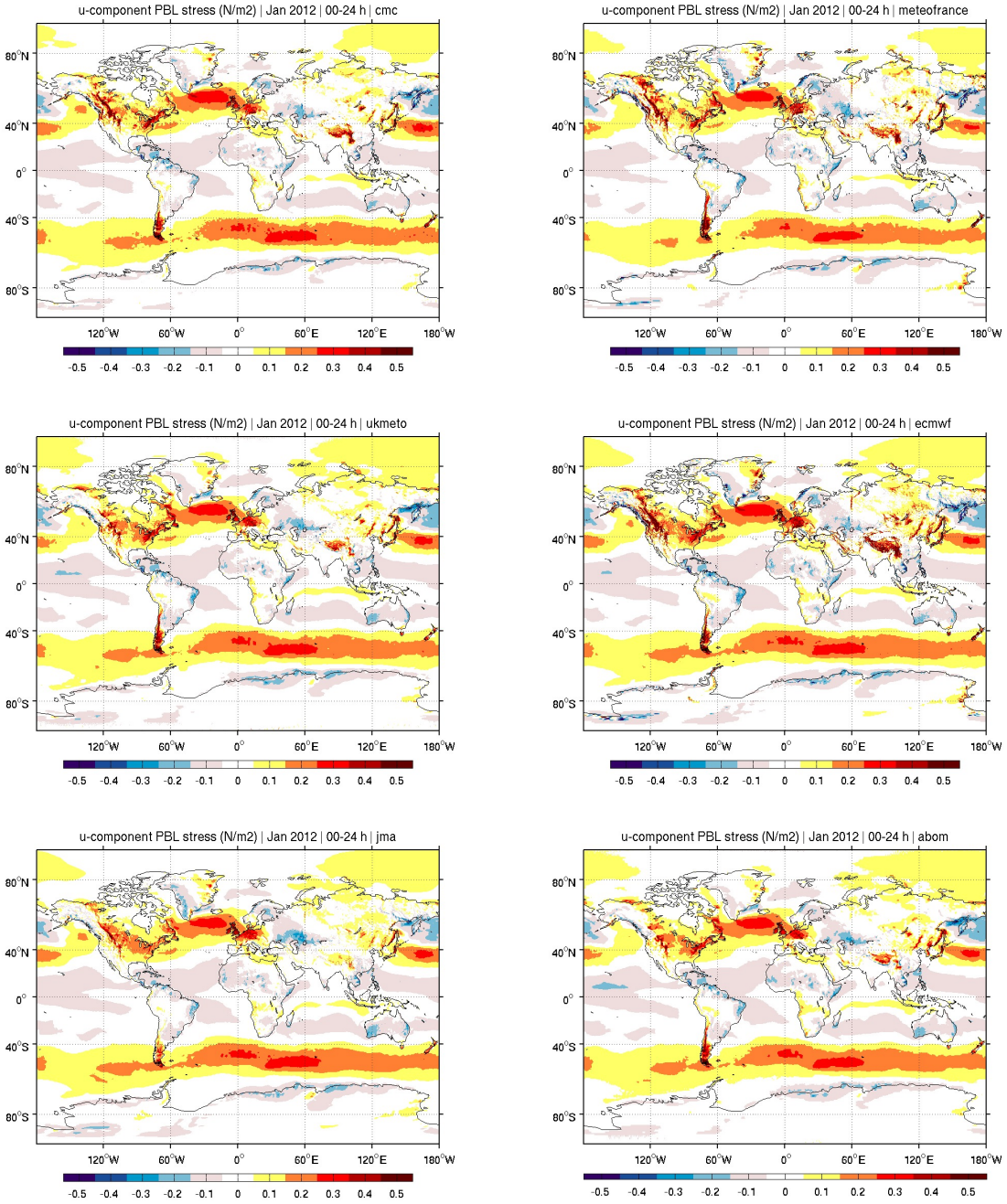

Figure 5: Same as in fig.1, for the PBL stress.

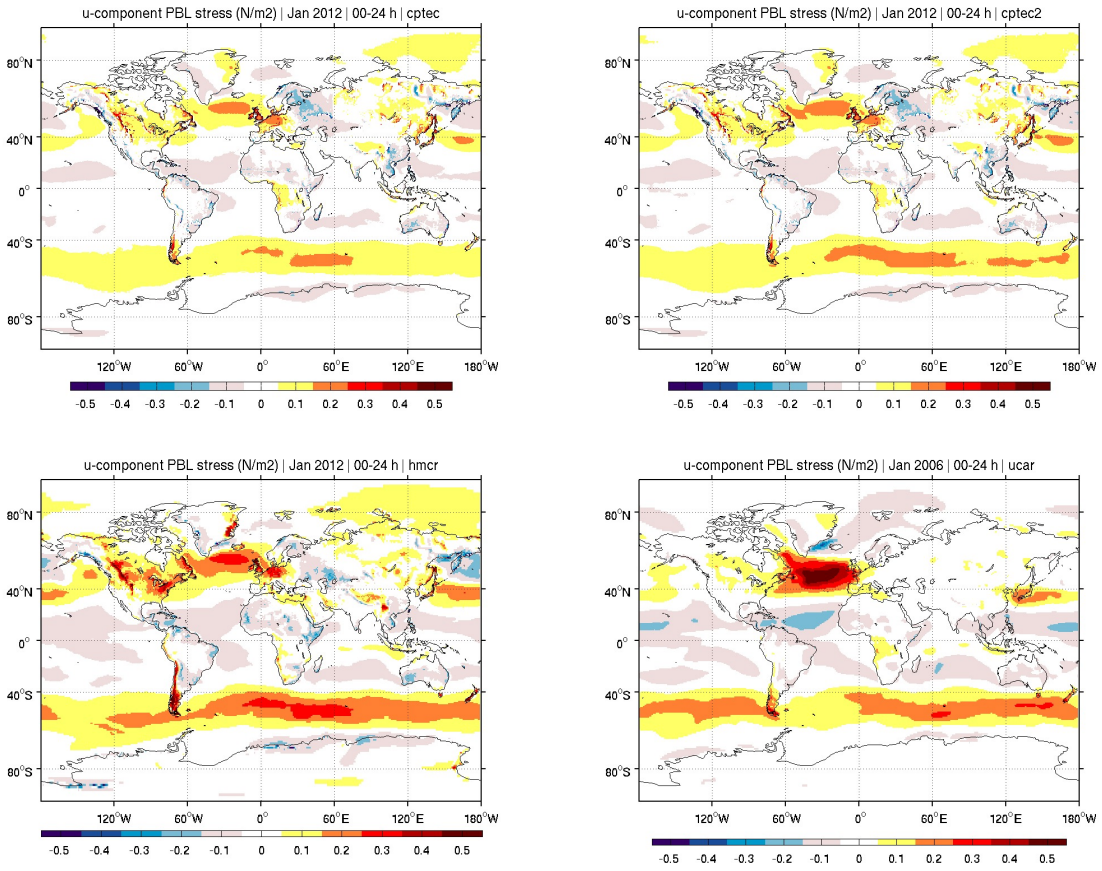

Figure 6: Same as in fig.5, for 4 more models.

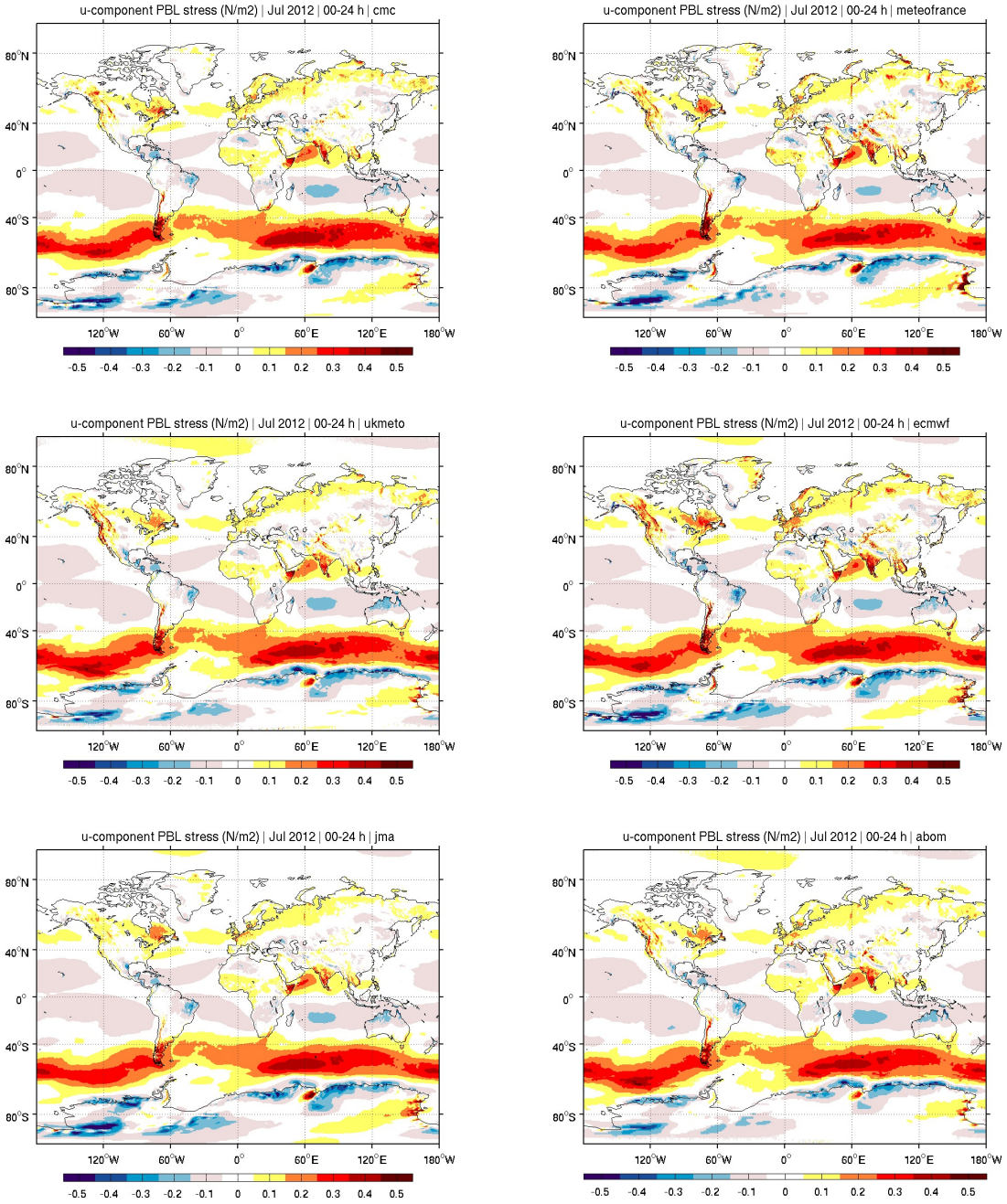

Figure 7: Same as in fig.3, for the PBL stress.

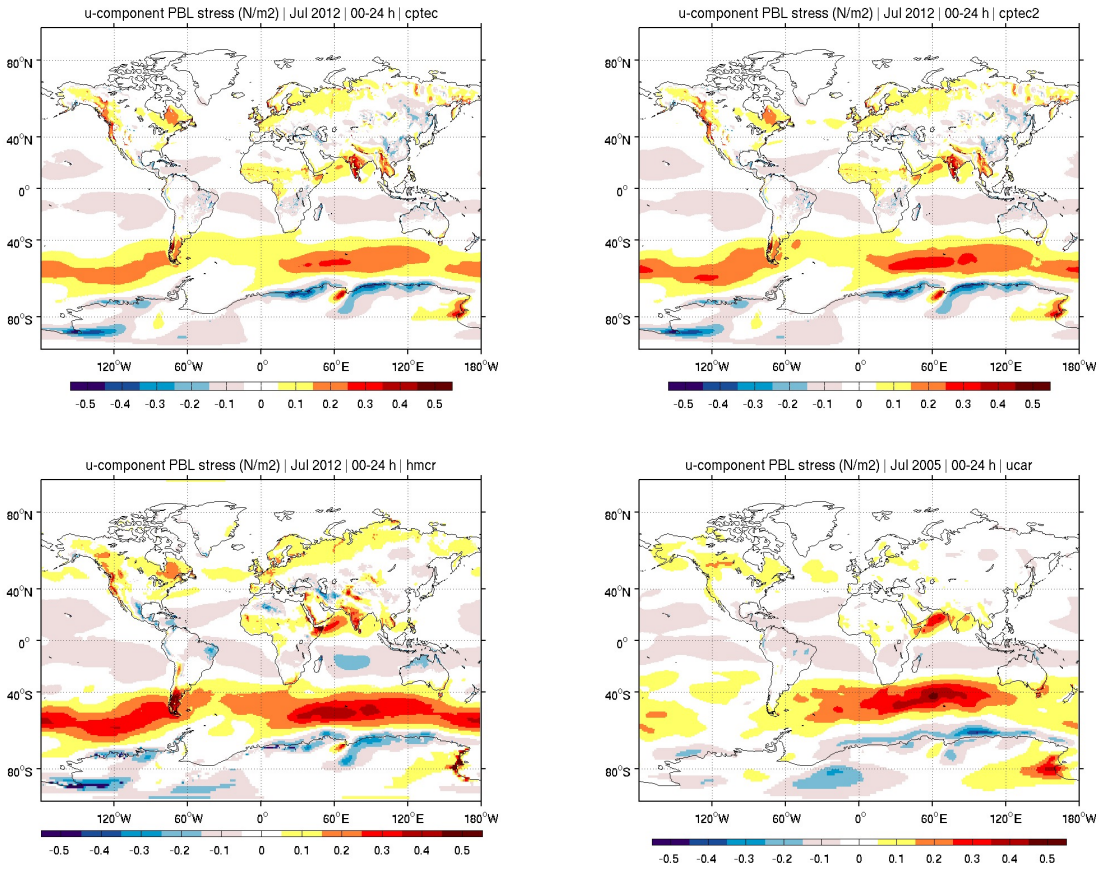

Figure 8: Same as in fig.7, for 4 more models.

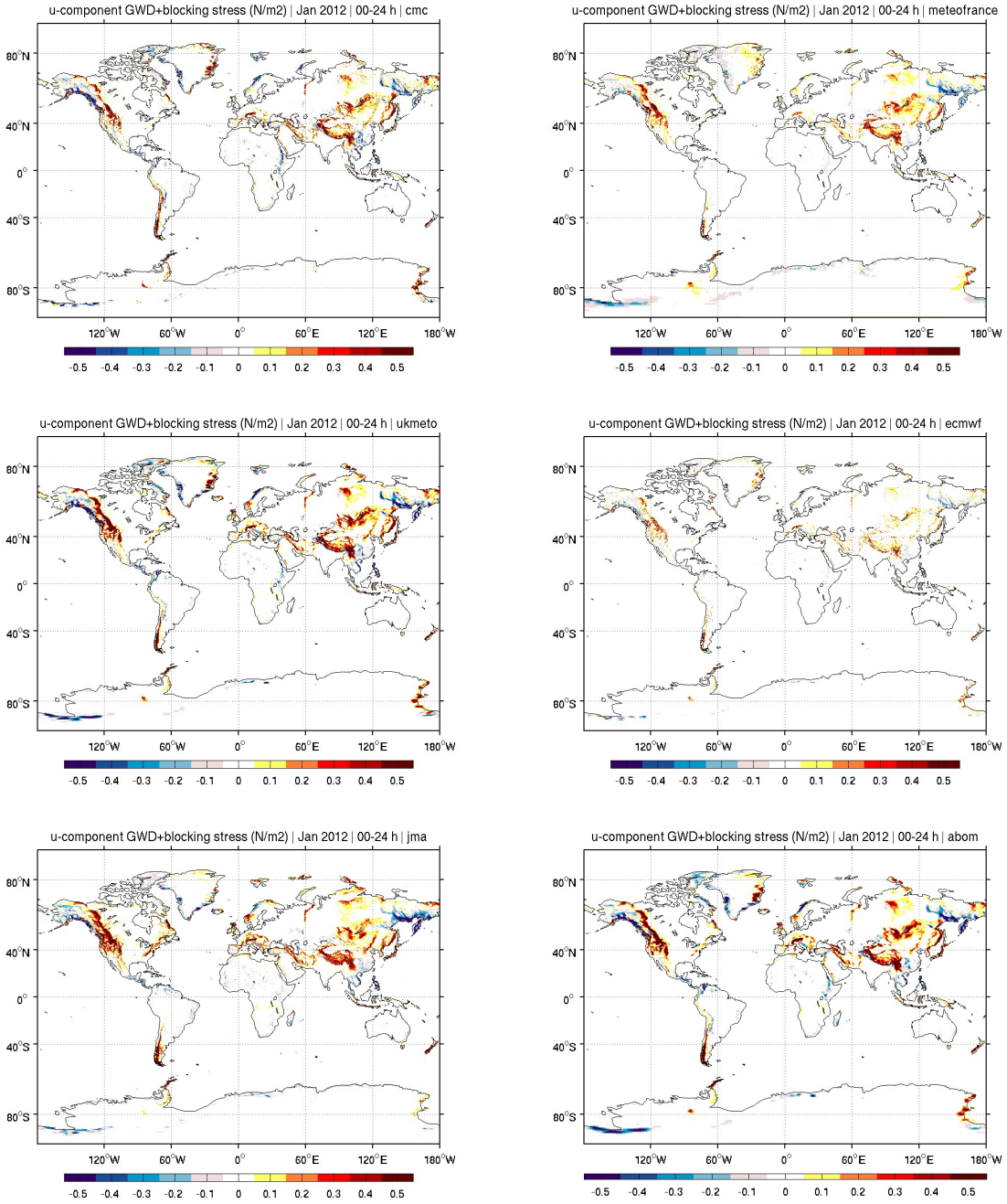

Figure 9: Same as in fig.1, for the SGO stress.

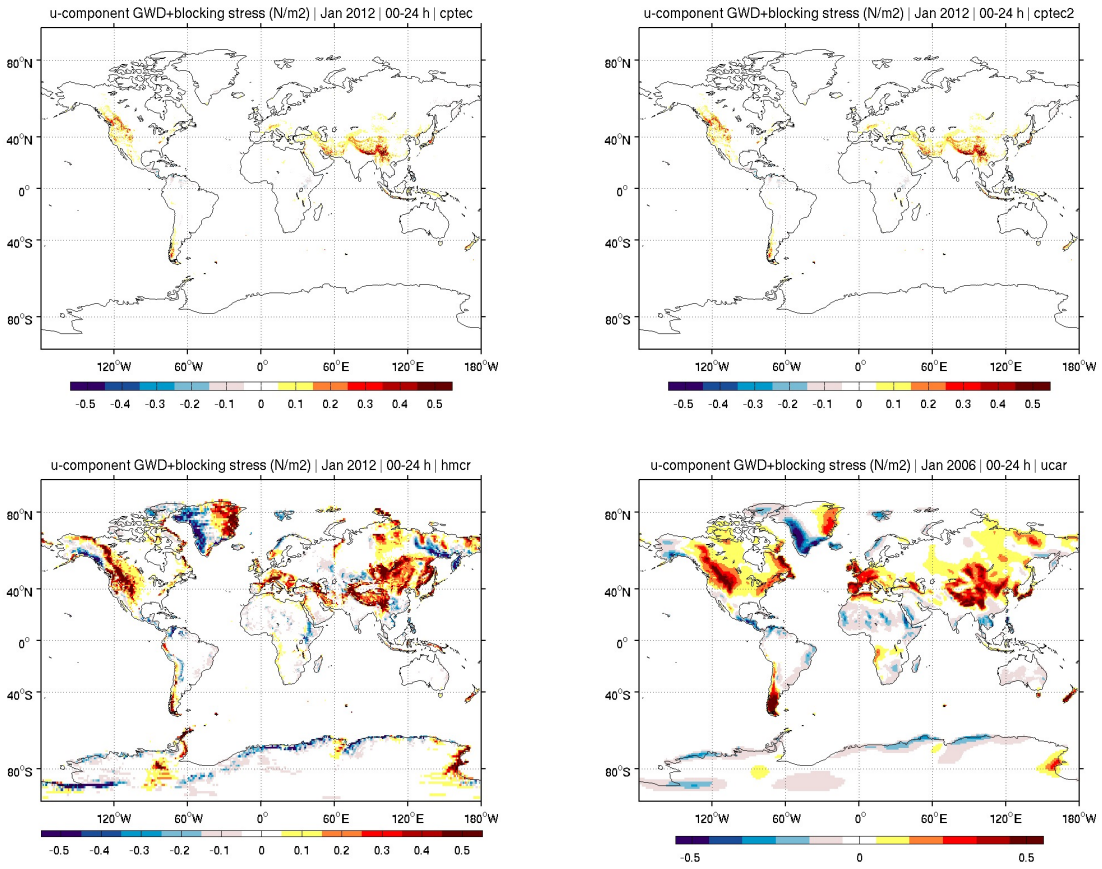

Figure 10: Same as in fig.9, for 4 more models.

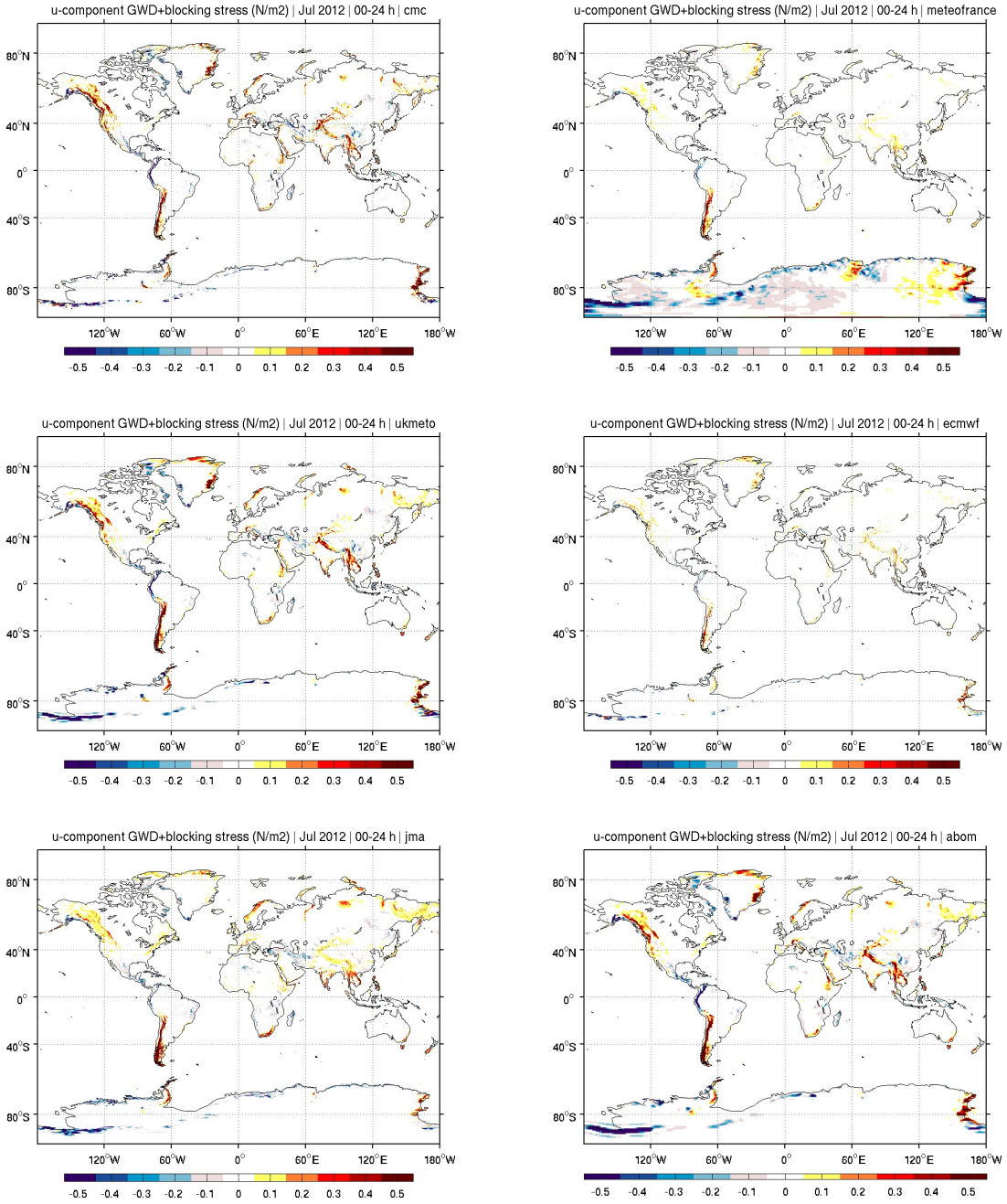

Figure 11: Same as in fig.3, for the SGO stress.

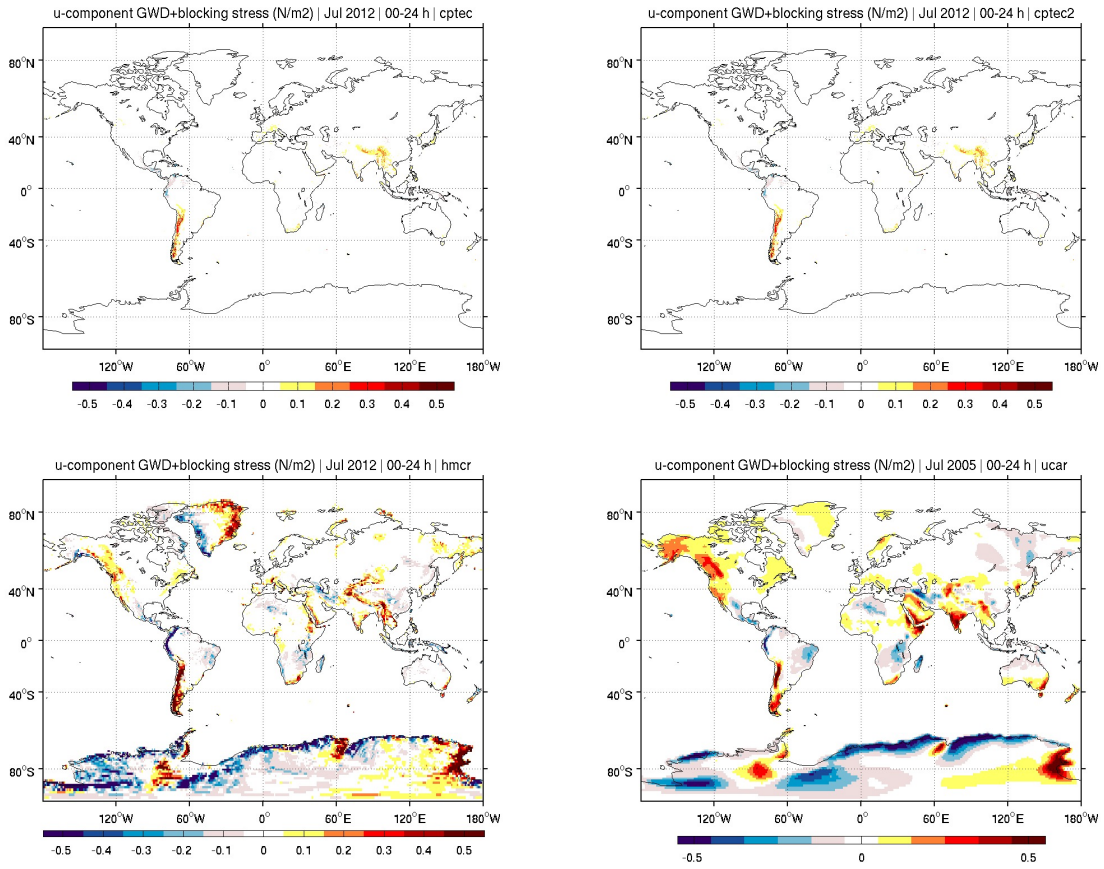

Figure 12: Same as in fig.11, for 4 more models.

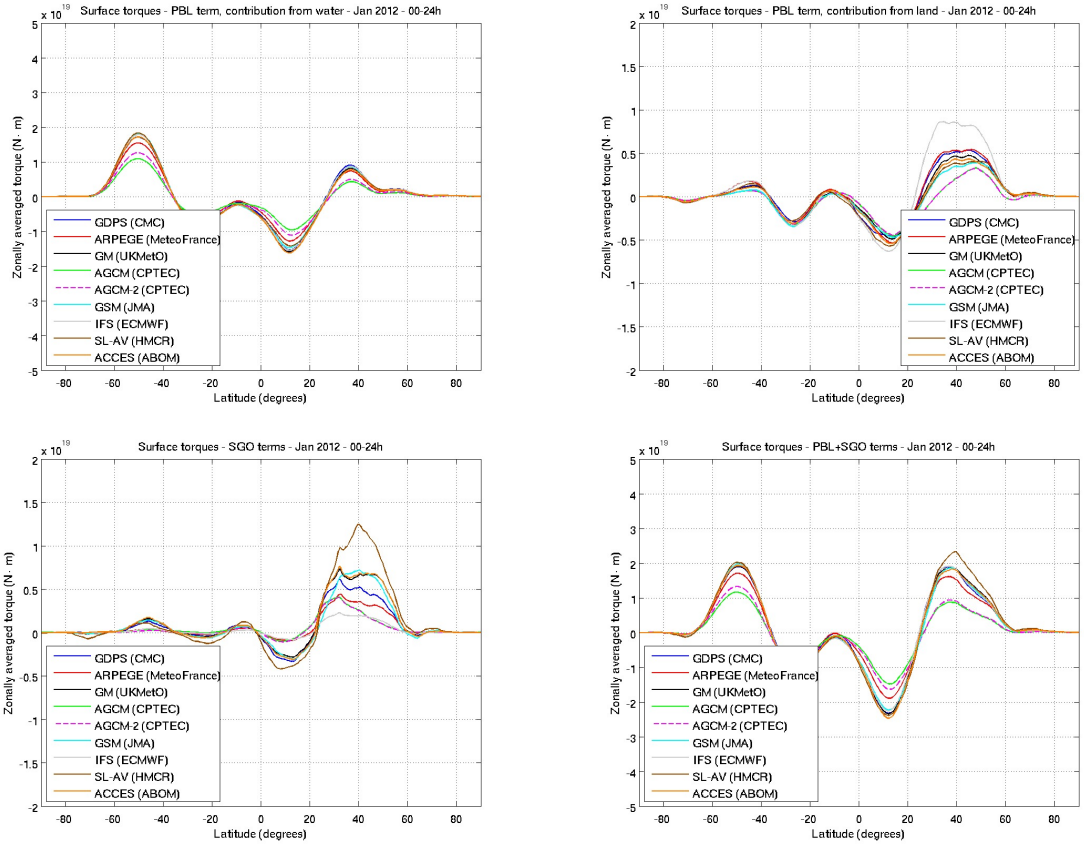

Figure 13: Zonal averages of surface torques in $(N \cdot m)$, using 00-24 UTC averages from Jan 2012: PBL contribution from water (top left), PBL contribution from land (top right), SGO contribution (bottom left), and total torque from the physics (bottom right).

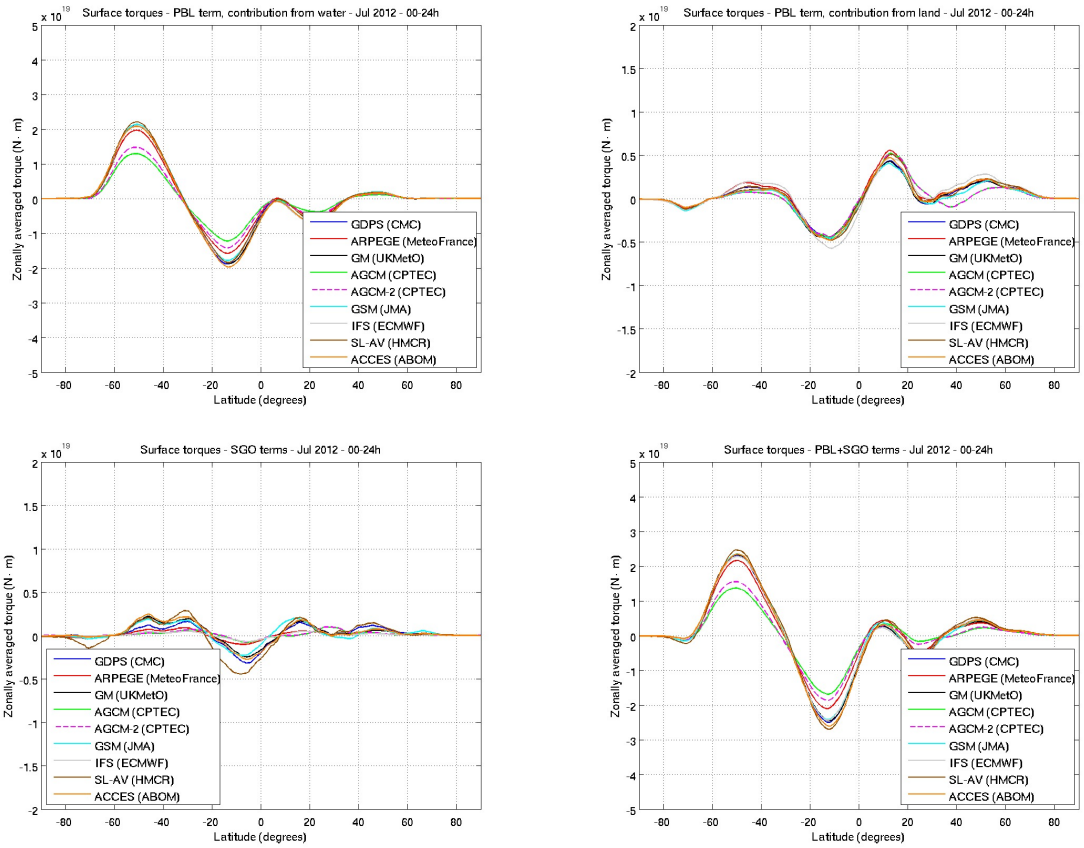

Figure 14: Same as fig.13, for Jul 2012.

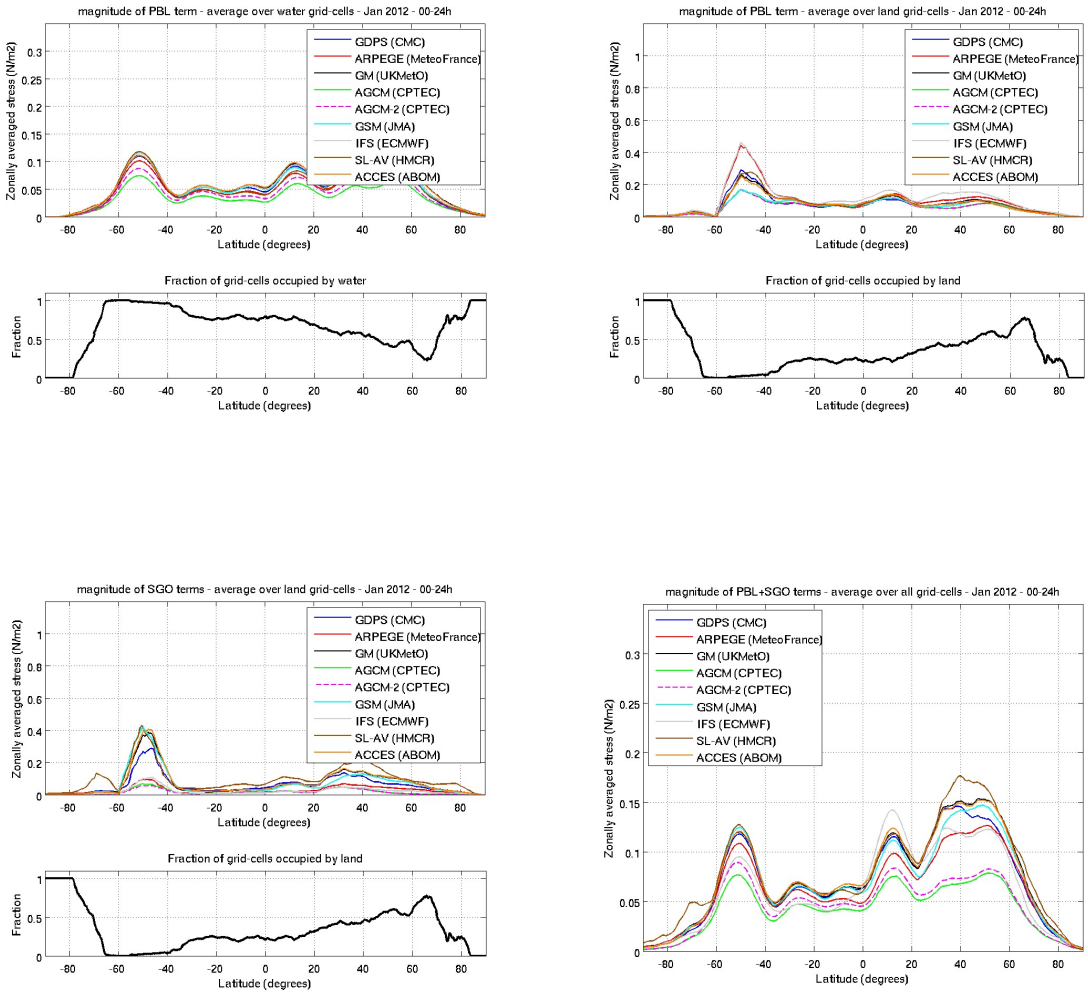

Figure 15: Zonal averages of the surface stress magnitude, using 00-24 UTC averages from Jan 2012: PBL contribution over water grid cells (top left), PBL contribution over land grid cells (top right), SGO contribution (bottom left), and physics stress over all grid cells (bottom right).

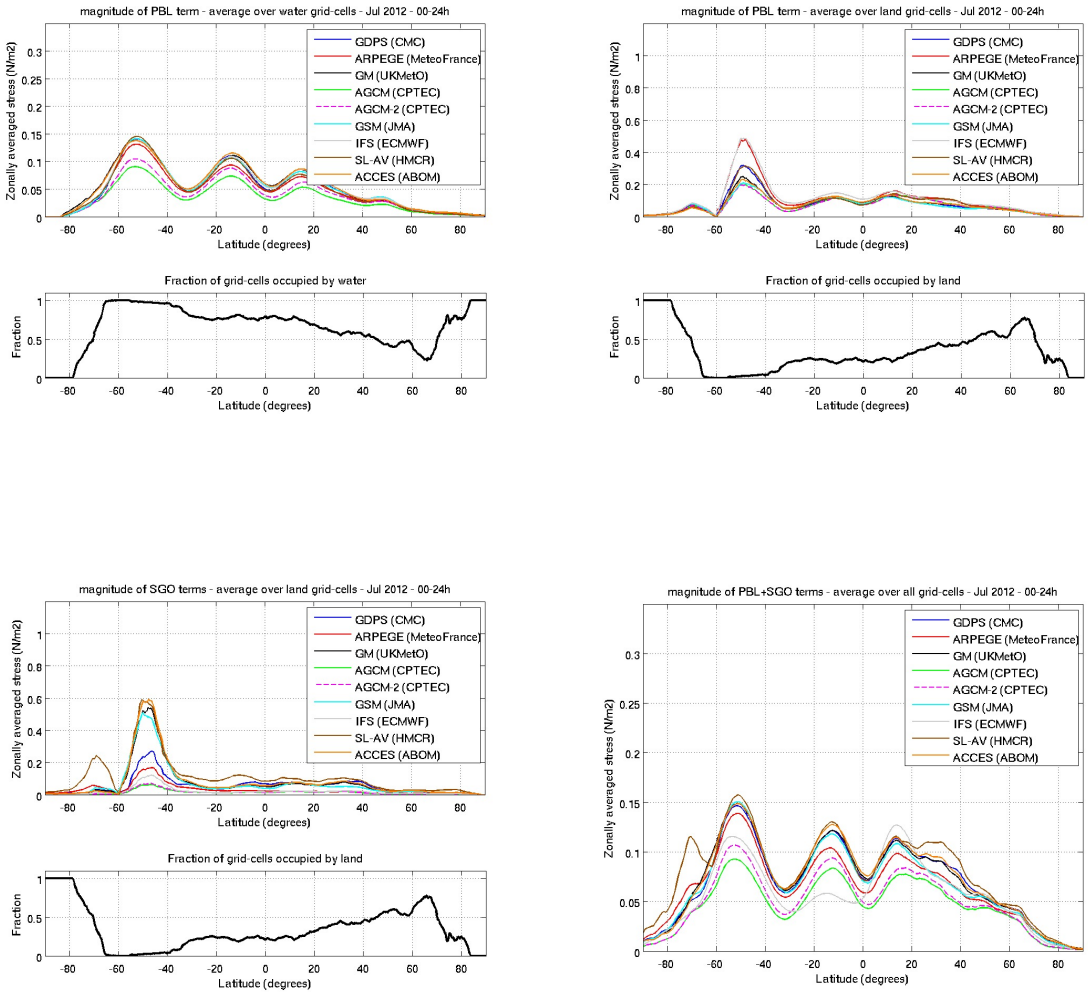

Figure 16: Same as fig.15, for Jul 2012.

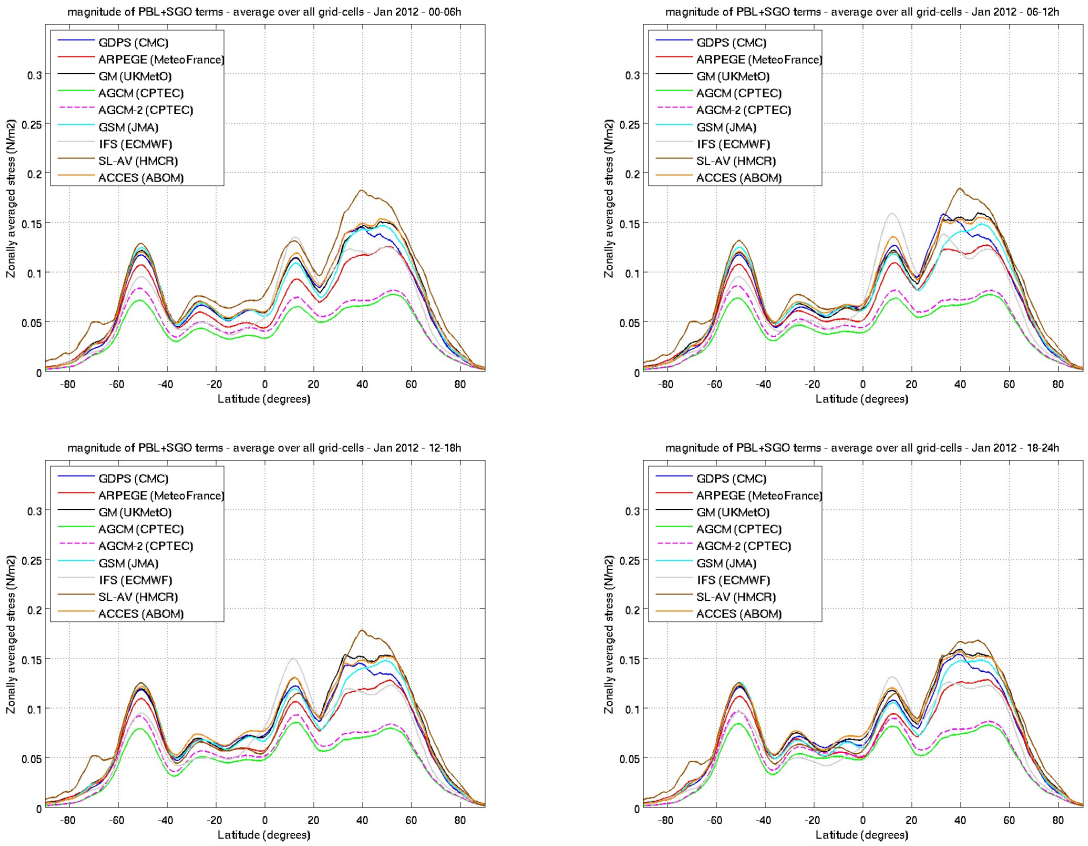

Figure 17: Example of diurnal cycle of surface torque: contribution from the physics to the torque over stress magnitude (in Nm^{-1}) for Jan 2012, averaged over the 00-06 (top left), 06-12 (to right), 12-18 (bottom left) amd 18-24 UTC interval (bottom right).